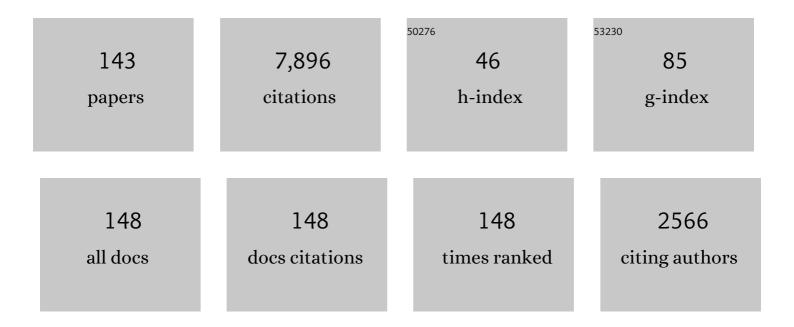
Michael G Henderson

List of Publications by Year in descending order

Source: https://exaly.com/author-pdf/9563343/publications.pdf Version: 2024-02-01



#	Article	IF	CITATIONS
1	Generation of Subauroral Longitudinally Extended Emissions Following Intensifications of the Poleward Boundary of the Substorm Bulge and Streamer Production. Journal of Geophysical Research: Space Physics, 2021, 126, e2020JA028556.	2.4	4
2	Magnetotail Dipolarizations and Ion Flux Variations During the Main Phase of Magnetic Storms. Journal of Geophysical Research: Space Physics, 2021, 126, e2020JA028470.	2.4	8
3	Geospace Plume and Its Impact on Dayside Magnetopause Reconnection Rate. Journal of Geophysical Research: Space Physics, 2021, 126, e2021JA029117.	2.4	7
4	Key elements of auroral substorm development and their relationship to recent observations of detached sub-auroral phenomena including STEVE-like emissions. Journal of Atmospheric and Solar-Terrestrial Physics, 2021, 218, 105600.	1.6	3
5	The impact of cold electrons and cold ions in magnetospheric physics. Journal of Atmospheric and Solar-Terrestrial Physics, 2021, 220, 105599.	1.6	27
6	Topological Segmentation and Tracking for Space Weather Modeling. , 2021, , .		0
7	Why Are There so Few Reports of Highâ€Energy Electron Drift Resonances? Role of Radial Phase Space Density Gradients. Journal of Geophysical Research: Space Physics, 2020, 125, e2020JA027924.	2.4	8
8	Defining Radiation Belt Enhancement Events Based on Probability Distributions. Space Weather, 2020, 18, e2020SW002528.	3.7	4
9	Calculating Ionizing Doses in Geosynchronous Orbit from In-situ Particle Measurements and Models. , 2020, , .		1
10	A Mission Concept to Determine the Magnetospheric Causes of Aurora. Frontiers in Astronomy and Space Sciences, 2020, 7, .	2.8	8
11	Physical Processes of Meso-Scale, Dynamic Auroral Forms. Space Science Reviews, 2020, 216, 1.	8.1	23
12	Solving the auroral-arc-generator question by using an electron beam to unambiguously connect critical magnetospheric measurements to auroral images. Journal of Atmospheric and Solar-Terrestrial Physics, 2020, 206, 105310.	1.6	11
13	How whistler mode hiss waves and the plasmasphere drive the quiet decay of radiation belts electrons following a geomagnetic storm. Journal of Physics: Conference Series, 2020, 1623, 012005.	0.4	8
14	On-orbit calibration of geostationary electron and proton flux observations for augmentation of an existing empirical radiation model. Journal of Space Weather and Space Climate, 2020, 10, 28.	3.3	5
15	The Cold Ion Population at Geosynchronous Orbit and Transport to the Dayside Magnetopause: September 2015 to February 2016. Journal of Geophysical Research: Space Physics, 2019, 124, 8685-8694.	2.4	4
16	The March 2015 Superstorm Revisited: Phase Space Density Profiles and Fast ULF Wave Diffusive Transport. Journal of Geophysical Research: Space Physics, 2019, 124, 1143-1156.	2.4	21
17	Improved Simulations of The Inner Magnetosphere During High Geomagnetic Activity With the RAM‧CB Model. Journal of Geophysical Research: Space Physics, 2019, 124, 4233-4248.	2.4	8
18	Extension of an Empirical Electron Flux Model From 6 to 20 Earth Radii Using Cluster/RAPID Observations. Space Weather, 2019, 17, 778-792.	3.7	11

#	Article	IF	CITATIONS
19	PreMevE: New Predictive Model for Megaelectronâ€Volt Electrons Inside Earth's Outer Radiation Belt. Space Weather, 2019, 17, 438-454.	3.7	24
20	Effects of a Realistic O ⁺ Source on Modeling the Ring Current. Journal of Geophysical Research: Space Physics, 2019, 124, 9953-9962.	2.4	5
21	Observations and Fokkerâ€Planck Simulations of the <i>L</i> â€Shell, Energy, and Pitch Angle Structure of Earth's Electron Radiation Belts During Quiet Times. Journal of Geophysical Research: Space Physics, 2019, 124, 1125-1142.	2.4	37
22	SAPSâ€Associated Explosive Brightening on the Duskside: A New Type of Onset‣ike Disturbance. Journal of Geophysical Research: Space Physics, 2018, 123, 197-210.	2.4	10
23	Particle tracing modeling of ion fluxes at geosynchronous orbit. Journal of Atmospheric and Solar-Terrestrial Physics, 2018, 177, 131-140.	1.6	3
24	Fast Diffusion of Ultrarelativistic Electrons in the Outer Radiation Belt: 17 March 2015 Storm Event. Geophysical Research Letters, 2018, 45, 10874-10882.	4.0	49
25	Calculation of Last Closed Drift Shells for the 2013 GEM Radiation Belt Challenge Events. Journal of Geophysical Research: Space Physics, 2018, 123, 9597-9611.	2.4	27
26	A Statistical Survey of Radiation Belt Dropouts Observed by Van Allen Probes. Geophysical Research Letters, 2018, 45, 8035-8043.	4.0	49
27	Energetic Particle Data From the Global Positioning System Constellation. Space Weather, 2017, 15, 283-289.	3.7	46
28	Simultaneous eventâ€specific estimates of transport, loss, and source rates for relativistic outer radiation belt electrons. Journal of Geophysical Research: Space Physics, 2017, 122, 3354-3373.	2.4	18
29	Investigating the source of nearâ€relativistic and relativistic electrons in Earth's inner radiation belt. Journal of Geophysical Research: Space Physics, 2017, 122, 695-710.	2.4	48
30	The Evolution of the Plasma Sheet Ion Composition: Storms and Recoveries. Journal of Geophysical Research: Space Physics, 2017, 122, 12,040.	2.4	12
31	Global Threeâ€Dimensional Simulation of Earth's Dayside Reconnection Using a Twoâ€Way Coupled Magnetohydrodynamics With Embedded Particleâ€inâ€Cell Model: Initial Results. Journal of Geophysical Research: Space Physics, 2017, 122, 10,318.	2.4	62
32	The plasma environment inside geostationary orbit: A Van Allen Probes HOPE survey. Journal of Geophysical Research: Space Physics, 2017, 122, 9207-9227.	2.4	34
33	Simulation of energyâ€dependent electron diffusion processes in the Earth's outer radiation belt. Journal of Geophysical Research: Space Physics, 2016, 121, 4217-4231.	2.4	50
34	The Global Positioning System constellation as a space weather monitor: Comparison of electron measurements with Van Allen Probes data. Space Weather, 2016, 14, 76-92.	3.7	48
35	Reproducing the observed energyâ€dependent structure of Earth's electron radiation belts during storm recovery with an eventâ€specific diffusion model. Geophysical Research Letters, 2016, 43, 5616-5625.	4.0	71
36	Recurrent embedded substorms during the 19 October 1998 GEM storm. Journal of Geophysical Research: Space Physics, 2016, 121, 7847-7859.	2.4	6

#	Article	IF	CITATIONS
37	The latitudinal variation of geoelectromagnetic disturbances during large (<i>Dst</i> â‰≇'100ÂnT) geomagnetic storms. Space Weather, 2016, 14, 668-681.	3.7	23
38	Highly relativistic radiation belt electron acceleration, transport, and loss: Large solar storm events of March and June 2015. Journal of Geophysical Research: Space Physics, 2016, 121, 6647-6660.	2.4	93
39	An improved empirical model of electron and ion fluxes at geosynchronous orbit based on upstream solar wind conditions. Space Weather, 2016, 14, 511-523.	3.7	42
40	Ring current pressure estimation with RAM CB using data assimilation and Van Allen Probe flux data. Geophysical Research Letters, 2016, 43, 11,948.	4.0	14
41	The complex nature of storm-time ion dynamics: Transport and local acceleration. Geophysical Research Letters, 2016, 43, 10,059-10,067.	4.0	17
42	Forecasting and remote sensing outer belt relativistic electrons from low Earth orbit. Geophysical Research Letters, 2016, 43, 1031-1038.	4.0	14
43	Observations of the impenetrable barrier, the plasmapause, and the VLF bubble during the 17 March 2015 storm. Journal of Geophysical Research: Space Physics, 2016, 121, 5537-5548.	2.4	59
44	Determination of errors in derived magnetic field directions in geosynchronous orbit: results from a statistical approach. Annales Geophysicae, 2016, 34, 831-843.	1.6	2
45	An empirical model of electron and ion fluxes derived from observations at geosynchronous orbit. Space Weather, 2015, 13, 233-249.	3.7	44
46	Empirical modeling of 3â€D forceâ€balanced plasma and magnetic field structures during substorm growth phase. Journal of Geophysical Research: Space Physics, 2015, 120, 6496-6513.	2.4	29
47	A background correction algorithm for Van Allen Probes MagEIS electron flux measurements. Journal of Geophysical Research: Space Physics, 2015, 120, 5703-5727.	2.4	78
48	Relativistic electron response to the combined magnetospheric impact of a coronal mass ejection overlapping with a highâ€speed stream: Van Allen Probes observations. Journal of Geophysical Research: Space Physics, 2015, 120, 7629-7641.	2.4	17
49	Modeling inward diffusion and slow decay of energetic electrons in the Earth's outer radiation belt. Geophysical Research Letters, 2015, 42, 987-995.	4.0	87
50	A 2-D empirical plasma sheet pressure model for substorm growth phase using the Support Vector Regression Machine. Journal of Geophysical Research: Space Physics, 2015, 120, 1957-1973.	2.4	10
51	Acceleration and loss driven by VLF chorus: Van Allen Probes observations and DREAM model results. , 2014, , .		0
52	On the cause and extent of outer radiation belt losses during the 30 September 2012 dropout event. Journal of Geophysical Research: Space Physics, 2014, 119, 1530-1540.	2.4	110
53	Competing source and loss mechanisms due to waveâ€particle interactions in Earth's outer radiation belt during the 30 September to 3 October 2012 geomagnetic storm. Journal of Geophysical Research: Space Physics, 2014, 119, 1960-1979.	2.4	103
54	REPAD: An empirical model of pitch angle distributions for energetic electrons in the Earth's outer radiation belt. Journal of Geophysical Research: Space Physics, 2014, 119, 1693-1708.	2.4	37

#	Article	IF	CITATIONS
55	The trapping of equatorial magnetosonic waves in the Earth's outer plasmasphere. Geophysical Research Letters, 2014, 41, 6307-6313.	4.0	51
56	Van Allen Probes observations of direct waveâ€particle interactions. Geophysical Research Letters, 2014, 41, 1869-1875.	4.0	32
57	Current sheet scattering and ion isotropic boundary under 3â€D empirical forceâ€balanced magnetic field. Journal of Geophysical Research: Space Physics, 2014, 119, 8202-8211.	2.4	22
58	Modeling gradual diffusion changes in radiation belt electron phase space density for the March 2013 Van Allen Probes case study. Journal of Geophysical Research: Space Physics, 2014, 119, 8396-8403.	2.4	24
59	Gradual diffusion and punctuated phase space density enhancements of highly relativistic electrons: Van Allen Probes observations. Geophysical Research Letters, 2014, 41, 1351-1358.	4.0	127
60	Data assimilation of space-based and ground-based observations, and empirical models into a plasmasphere model. , 2014, , .		0
61	The Magnetic Electron Ion Spectrometer (MagEIS) Instruments Aboard the Radiation Belt Storm Probes (RBSP) Spacecraft. Space Science Reviews, 2013, 179, 383-421.	8.1	491
62	Electron Acceleration in the Heart of the Van Allen Radiation Belts. Science, 2013, 341, 991-994.	12.6	463
63	Rapid local acceleration of relativistic radiation-belt electrons by magnetospheric chorus. Nature, 2013, 504, 411-414.	27.8	608
64	Van Allen Probes observation of localized drift resonance between poloidal mode ultraâ€low frequency waves and 60 keV electrons. Geophysical Research Letters, 2013, 40, 4491-4497.	4.0	127
65	Science Goals and Overview of the Radiation Belt Storm Probes (RBSP) Energetic Particle, Composition, and Thermal Plasma (ECT) Suite on NASA's Van Allen Probes Mission. Space Science Reviews, 2013, 179, 311-336.	8.1	463
66	Phase Space Density matching of relativistic electrons using the Van Allen Probes: REPT results. Geophysical Research Letters, 2013, 40, 4798-4802.	4.0	27
67	Evolution and slow decay of an unusual narrow ring of relativistic electrons near L ~ 3.2 following the September 2012 magnetic storm. Geophysical Research Letters, 2013, 40, 3507-3511.	4.0	150
68	A Long-Lived Relativistic Electron Storage Ring Embedded in Earth's Outer Van Allen Belt. Science, 2013, 340, 186-190.	12.6	216
69	Statistical properties of the surfaceâ€charging environment at geosynchronous orbit. Space Weather, 2013, 11, 237-244.	3.7	62
70	Helium, Oxygen, Proton, and Electron (HOPE) Mass Spectrometer for the Radiation Belt Storm Probes Mission. Space Science Reviews, 2013, 179, 423-484.	8.1	459
71	Modeling radiation belt electron dynamics during GEM challenge intervals with the DREAM3D diffusion model. Journal of Geophysical Research: Space Physics, 2013, 118, 6197-6211.	2.4	111
72	"Snowplow―injection front effects. Journal of Geophysical Research: Space Physics, 2013, 118, 6478-6488.	2.4	6

#	Article	IF	CITATIONS
73	Helium, Oxygen, Proton, and Electron (HOPE) Mass Spectrometer for the Radiation Belt Storm Probes Mission. , 2013, , 423-484.		13
74	Science Goals and Overview of the Radiation Belt Storm Probes (RBSP) Energetic Particle, Composition, and Thermal Plasma (ECT) Suite on NASA's Van Allen Probes Mission. , 2013, , 311-336.		8
75	Energetic particle injections to geostationary orbit: Relationship to flow bursts and magnetospheric state. Journal of Geophysical Research, 2012, 117, .	3.3	63
76	Dynamic Radiation Environment Assimilation Model: DREAM. Space Weather, 2012, 10, .	3.7	74
77	On the relationship between relativistic electron flux and solar wind velocity: Paulikas and Blake revisited. Journal of Geophysical Research, 2011, 116, n/a-n/a.	3.3	148
78	Startâ€ŧoâ€end global imaging of a sunward propagating, SAPSâ€associated giant undulation event. Journal of Geophysical Research, 2010, 115, .	3.3	27
79	Comment on "Investigation of the period of sawtooth events―by X. Cai and C. R. Clauer. Journal of Geophysical Research, 2010, 115, .	3.3	3
80	SpacePy - A Python-based Library of Tools for the Space Sciences. , 2010, , .		36
81	Plasma in Saturn's nightside magnetosphere and the implications for global circulation. Planetary and Space Science, 2009, 57, 1714-1722.	1.7	85
82	Northward field excursions in Saturn's magnetotail and their relationship to magnetospheric periodicities. Geophysical Research Letters, 2009, 36, .	4.0	41
83	Thermal ion flow in Saturn's inner magnetosphere measured by the Cassini plasma spectrometer: A signature of the Enceladus torus?. Geophysical Research Letters, 2009, 36, .	4.0	68
84	Observational evidence for an inside-out substorm onset scenario. Annales Geophysicae, 2009, 27, 2129-2140.	1.6	81
85	Magnetospheric solitary structure maintained by 3000 km/s ions as a cause of westward moving auroral bulge at 19 MLT. Annales Geophysicae, 2009, 27, 2947-2969.	1.6	6
86	Plasmoids in Saturn's magnetotail. Journal of Geophysical Research, 2008, 113, .	3.3	79
87	Nearâ€Earth substorm features from multiple satellite observations. Journal of Geophysical Research, 2008, 113, .	3.3	26
88	Highly periodic stormtime activations observed by THEMIS prior to substorm onset. Geophysical Research Letters, 2008, 35, .	4.0	3
89	Cassini detection of waterâ€group pickâ€up ions in the Enceladus torus. Geophysical Research Letters, 2008, 35, .	4.0	47
90	Cassini plasma spectrometer thermal ion measurements in Saturn's inner magnetosphere. Journal of Geophysical Research, 2008, 113, .	3.3	120

#	Article	IF	CITATIONS
91	Rice Convection Model simulation of the 18 April 2002 sawtooth event and evidence for interchange instability. Journal of Geophysical Research, 2008, 113, .	3.3	21
92	Transport of plasma sheet material to the inner magnetosphere. Geophysical Research Letters, 2007, 34,	4.0	15
93	Comparative statistical analysis of storm time activations and sawtooth events. Journal of Geophysical Research, 2007, 112, n/a-n/a.	3.3	46
94	Cluster observations in the inner magnetosphere during the 18 April 2002 sawtooth event: Dipolarization and injection at <i>r</i> = 4.6 <i>R</i> _{<i>E</i>} . Journal of Geophysical Research, 2007, 112, .	3.3	40
95	Observations of dipolarization at geosynchronous orbits and its response in the polar cap convection during extreme southward interplanetary magnetic field conditions. Journal of Geophysical Research, 2007, 112, .	3.3	1
96	Prelude to THEMIS tail conjunction study. Annales Geophysicae, 2007, 25, 1001-1009.	1.6	6
97	Key features of intense geospace storms—A comparative study of a solar maximum and a solar minimum storm. Planetary and Space Science, 2007, 55, 32-52.	1.7	9
98	Modeling the ring current response to a sawtooth oscillation event. Journal of Atmospheric and Solar-Terrestrial Physics, 2007, 69, 67-76.	1.6	9
99	Global auroral imaging in the ILWS era. Advances in Space Research, 2007, 40, 409-418.	2.6	5
100	Characterizing the 18 April 2002 storm-time sawtooth events using ground magnetic data. Journal of Geophysical Research, 2006, 111, .	3.3	50
101	Magnetospheric and auroral activity during the 18 April 2002 sawtooth event. Journal of Geophysical Research, 2006, 111, .	3.3	100
102	Unusually quick development of a 4000 nT substorm during the initial 10 min of the 29 October 2003 magnetic storm. Journal of Geophysical Research, 2006, 111, .	3.3	10
103	Substorms during the $10\hat{a}\in$ "11 August 2000 sawtooth event. Journal of Geophysical Research, 2006, 111, .	3.3	69
104	Geomagnetic storms driven by ICME- and CIR-dominated solar wind. Journal of Geophysical Research, 2006, 111, .	3.3	199
105	Analyzing electric field morphology through data-model comparisons of the Geospace Environment Modeling Inner Magnetosphere/Storm Assessment Challenge events. Journal of Geophysical Research, 2006, 111, .	3.3	37
106	A statistical study of magnetic dipolarization for sawtooth events and isolated substorms at geosynchronous orbit with GOES data. Annales Geophysicae, 2006, 24, 3481-3490.	1.6	29
107	Toward understanding radiation belt dynamics, nuclear explosion-produced artificial belts, and active radiation belt remediation: Producing a radiation belt data assimilation model. Geophysical Monograph Series, 2005, , 221-235.	0.1	7
108	Cluster magnetotail observations of a tailward-travelling plasmoid at substorm expansion phase onset and field aligned currents in the plasma sheet boundary layer. Annales Geophysicae, 2005, 23, 3667-3683.	1.6	7

#	Article	IF	CITATIONS
109	Calculation of IMAGE/MENA geometric factors and conversion of images to units of integral and differential flux. Review of Scientific Instruments, 2005, 76, 043303.	1.3	11
110	Storm-time plasma signatures observed by IMAGE/MENA and comparison with a global physics-based model. Geophysical Research Letters, 2005, 32, .	4.0	20
111	The May 2-3, 1986 CDAW-9C interval: A sawtooth event. Geophysical Research Letters, 2004, 31, n/a-n/a.	4.0	63
112	Magnetotail behavior during storm time "sawtooth injections― Journal of Geophysical Research, 2004, 109, .	3.3	31
113	Tail-dominated storm main phase: 31 March 2001. Journal of Geophysical Research, 2003, 108, .	3.3	29
114	IMAGE, POLAR, and geosynchronous observations of substorm and ring current ion injection. Geophysical Monograph Series, 2003, , 91-101.	0.1	52
115	O+ Transport into the ring current: Storm versus substorm. Geophysical Monograph Series, 2003, , 59-73.	0.1	12
116	The Role and Contributions of Energetic Neutral Atom (ENA) Imaging in Magnetospheric Substorm Research. , 2003, , 155-182.		2
117	Ps 6 disturbances: relation to substorms and the auroral oval. Annales Geophysicae, 2003, 21, 493-508.	1.6	16
118	Charge exchange contribution to the decay of the ring current, measured by energetic neutral atoms (ENAs). Journal of Geophysical Research, 2001, 106, 1931-1937.	3.3	26
119	Plasma sheet access to the inner magnetosphere. Journal of Geophysical Research, 2001, 106, 5845-5858.	3.3	58
120	The storm-substorm relationship: Ion injections in geosynchronous measurements and composite energetic neutral atom images. Journal of Geophysical Research, 2001, 106, 5833-5844.	3.3	62
121	First medium energy neutral atom (MENA) Images of Earth's magnetosphere during substorm and storm-time. Geophysical Research Letters, 2001, 28, 1147-1150.	4.0	61
122	Simultaneous closed magnetic field line polar arcs and substorms. Journal of Atmospheric and Solar-Terrestrial Physics, 2001, 63, 643-655.	1.6	3
123	Polar CEPPAD/IPS energetic neutral atom (ENA) images of a substorm injection. Advances in Space Research, 2000, 25, 2407-2416.	2.6	10
124	Association of energetic neutral atom bursts and magnetospheric substorms. Journal of Geophysical Research, 2000, 105, 18753-18763.	3.3	15
125	Energetic neutral atom imaging with the polar ceppad/ips instrument: Initial forward modeling results. Physics and Chemistry of the Earth, Part C: Solar, Terrestrial and Planetary Science, 1999, 24, 203-208.	0.2	3
126	The relativistic electron response at geosynchronous orbit during the January 1997 magnetic storm. Journal of Geophysical Research, 1998, 103, 17559-17570.	3.3	104

#	Article	IF	CITATIONS
127	Coronal mass ejections, magnetic clouds, and relativistic magnetospheric electron events: ISTP. Journal of Geophysical Research, 1998, 103, 17279-17291.	3.3	144
128	Are north-south aligned auroral structures an ionospheric manifestation of bursty bulk flows?. Geophysical Research Letters, 1998, 25, 3737-3740.	4.0	186
129	First energetic neutral atom images from Polar. Geophysical Research Letters, 1997, 24, 1167-1170.	4.0	101
130	Global energetic neutral atom (ENA) measurements and their association with theDstindex. Geophysical Research Letters, 1997, 24, 3173-3176.	4.0	53
131	Viking observations of a reverse convection cell developing in response to a northward turning of the interplanetary magnetic field. Geophysical Research Letters, 1996, 23, 809-812.	4.0	1
132	Observations of magnetospheric substorms occurring with no apparent solar wind/IMF trigger. Journal of Geophysical Research, 1996, 101, 10773-10791.	3.3	72
133	Observations of auroral substorms occurring together with preexisting "quiet time―auroral patterns. Journal of Geophysical Research, 1996, 101, 24621-24640.	3.3	13
134	Comparison of Viking onset locations with the predictions of the Thermal Catastrophe Model. Journal of Geophysical Research, 1995, 100, 21857-21872.	3.3	11
135	Special features of a substorm during high solar wind dynamic pressure. Journal of Geophysical Research, 1995, 100, 19095.	3.3	10
136	Interpretation of optical substorm onset observations. Journal of Atmospheric and Solar-Terrestrial Physics, 1993, 55, 1159-1170.	0.9	34
137	The auroral distribution and its mapping according to substorm phase. Journal of Atmospheric and Solar-Terrestrial Physics, 1993, 55, 1741-1762.	0.9	34
138	Long-term energetic-particle databases from geosynchronous and GPS orbits. , 0, , .		0
139	Substorm Associated Spikes in High Energy Particle Precipitation. Geophysical Monograph Series, 0, , 227-236.	0.1	10
140	Los Alamos Geosynchronous Space Weather Data for Radiation Belt Modeling. Geophysical Monograph Series, 0, , 237-240.	0.1	3
141	Observations of Changes to the Auroral Distribution Prior to Substorm Onset. Geophysical Monograph Series, 0, , 257-275.	0.1	31
142	Auroral Substorms, Poleward Boundary Activations, Auroral Streamers, Omega Bands, and Onset Precursor Activity. Geophysical Monograph Series, 0, , 39-54.	0.1	41
143	Association of Mesoscale Auroral Structures and Breakups With Energetic Particle Injections at Geosynchronous Orbit. Frontiers in Astronomy and Space Sciences, 0, 9, .	2.8	2